



Climate Modelling User Group

Deliverable 4.1

Exploiting CCI products in MIP experiments

Centres providing input: Met Office, MPI-M, IPSL, BSC

Version	Date	Status
0.1	29 July 2019	First input from partners of activity and results
0.5	12 Sept 2019	Input from BSC, IPSL, Met Office
1.0	30 Sept 2019	Submitted to ESA
1.1	19 Dec 2019	Input from partners to address ESA RIDv1
1.2	12 Feb 2020	Revised version for submission to ESA
1.3	13 Mar 2021	Update to 1.2 with input from MPI-M

CMUG CCI+ Deliverable

Reference: D4.1: Exploiting CCI products in MIP experiments

Submission date: April 2021

Version: 1.3



Max-Planck-Institut
für Meteorologie





CMUG CCI+ Deliverable 4.1

Exploiting CCI products in MIP experiments

Table of Contents

1. Purpose and scope of this report.....	4
2. CMUG approach for assessing quality in CCI products.....	4
3. Links between Task 4 and the CMIP projects.....	7
4. CMUG MIP experiments with CCI products	9
4.1 Evaluation of modelled system memory	9
4.2 Evaluation of model results considering observational uncertainty.....	17
4.3 Evaluation of model results considering the abstraction level of observational products	26
4.4 Optimal spatial and temporal scales for model evaluation.....	27
4.5 Evaluation of model results considering internal variability.....	28
4.6 Evaluation of model results considering a combination of sources of uncertainties.....	30
4.7 Skill assessment of the DCPD decadal predictions	33
4.8 Use LST products to develop and test simple models relating the LST versus air temperature (near surface) difference to vegetation moisture stress.....	37
4.9 Use CCI+ products and simple models developed in WP4.8 to evaluate performance of modelled LST versus air temperature, using multiple up-to-date land surface and Earth System models.....	39
4.10 Comparison of CCI products for studying vegetation variations with other satellite products and land surface models.....	41
4.11 Assess the land-surface interaction related biases in AMIP simulations with CCI and other products	43
5. References.....	45



Report on exploiting CCI products in MIP experiments

1. Purpose and scope of this report

This document is the first report on the outputs of the CMUG Model Inter Comparison (MIP) type experiments using data products from the CCI+ ECV projects. Its purpose is to provide feedback to ESA and the CCI teams on the suitability and application of CCI climate data products in climate models. This activity has eleven experiments (CMUG WPs 4.1 to 4.11) by four CMUG partners. These are all focused studies which use CMIP6 model output for the research (as opposed to conducting new model runs). Many data products from the CCI ECVs are included, and outputs from five of the new CCI+ ECVs are used (or will be when available). An overview of the key features of the experiments is given in Table 1.

2. CMUG approach for assessing quality in CCI products

This work is concerned with exploiting CCI products in MIP experiments, with the activity in CMUG WPs 4.1 to 4.6 on statistical analyses that evaluate facets of model behaviour in representing climate. They carefully target individual elements of uncertainty derived either from the climate system (e.g. internal variability, system memory) or the observations (e.g. levels of processing or scales of averaging) and then provide a framework for combining these. There is an emphasis on characterising and understanding uncertainty in these experiments to inform the CMUG work on the ESMValTool to include uncertainty in its evaluation process for the metrics of the ECVs in these experiments. CMUG WP 4.7 addresses the important issue relevant to the component of CMIP6 focusing on decadal prediction by applying multiple CCI/CCI+ atmospheric and marine ECVs to generate an assessment of the skill in decadal forecasting systems. CMUG WPs 4.8 to 4.10 focus on the application of CCI/CCI+ terrestrial ECVs to evaluate the physical basis of representation of biophysical land surface processes and assess their simulation in earth system model components. They use data from the CMIP6 archive to understand plant climate interactions, their representation in climate models and evaluate model performance and suggest areas for future model development. WP 4.11 will build on the process analysis undertaken elsewhere in CMUG and will apply several ECVs and other datasets to identify the drivers of biases in the state of the terrestrial surface and the fluxes generated by its interaction with the atmosphere. This will provide an assessment of the value of combining multiple ECVs with other data sources to assess the quality and identify areas for improvement in the atmospheric model component of CMIP.

The uncertainty characterisation accompanying the CCI ECV datasets is examined to understand its usefulness in the modelling studies. The different types of uncertainty characterisation (grid point, bias, statistical, variance, temporal/spatial, or other) provided by the CCI ECV teams and how it meets user requirements is commented on in this report.

CMUG CCI+ Deliverable

Reference: D4.1: Exploiting CCI products in MIP experiments

Submission date: April 2021

Version: 1.3



CMUG WP	EXPLOITING CCI PRODUCTS IN MIP EXPERIMENTS	CMUG LEAD	EXPERIMENT TYPE		CCI ECVS	OTHER ECVS
4.1	Evaluation of modelled system memory	MPI-M	Statistical analysis	4	Salinity, Snow, LST, SST, SI	
4.2	Evaluation of model results considering observational uncertainty	MPI-M	Statistical analysis	4	Salinity, Snow, LST, SST, SI	
4.3	Evaluation of model results considering the abstraction level of observational products	MPI-M	Statistical analysis	4	Salinity, Snow, LST, SST, SI	
4.4	Optimal spatial and temporal scales for model evaluation	MPI-M	Statistical analysis	4	Salinity, Snow, LST, SST, SI	
4.5	Evaluation of model results considering internal variability	MPI-M	Statistical analysis	4	Salinity, Snow, LST, SST, SI	
4.6	Evaluation of model results considering a combination of sources of uncertainties	MPI-M	Statistical analysis	4	Salinity, Snow, LST, SST, SI	
4.7	Skill assessment of the DCPD decadal predictions	BSC	Skill analysis	4	Sea Level, SST, Clouds	
4.8	Use LST products to develop and test simple models relating the LST versus air temperature (near surface) difference to vegetation moisture stress	Met Office	MIP process analysis	3	AGBiomass, LST, SM, LC	Temperature, Precipitation, FAPAR, LAI
4.9	Use CCI+ products and simple models developed in WP4.8 to evaluate performance of LST versus air temp, using multiple land surface and ES models	Met Office	MIP process analysis	3	LST, AGBiomass, LC/HRLC	Temperature

CMUG CCI+ Deliverable

Reference: **D4.1: Exploiting CCI products in MIP experiments**

Submission date: **April 2021**

Version: **1.3**



4.10	Comparison of CCI data in vegetation study with other satellite data and LS models	Met Office	MIP process analysis	3	AGBiomass, LST, SM, LC	Temperature, Precipitation, FAPAR, LAI
4.11	Land-surface interaction related biases in AMIP	IPSL	MIP process analysis	4	LST , Snow, SM	Air temp, turb. fluxes (Jung, Gleam,) meteo analysis, MODIS data, CERES rad. fluxes, SM (SMOS, Gleam)

Table 1: Main features of the work on exploiting CCI products in MIP experiments.



3. Links between Task 4 and the CMIP projects

The results are relevant to the CMIP6 endorsed MIP projects that are working in a similar research area to CMUG WP4. CMIP is part of WCRP (World Climate Research Programme) which has proposed areas for emphasis in climate research called the ‘grand challenges’¹, which the MIPs are helping to address. There are currently 23 CMIP6 endorsed MIP projects² (plus 17 related or supporting MIP type projects) which cover a wide range of Earth system processes and modelling activities. The CMUG partners working on this Task are engaging with relevant CMIP projects and exchanging results and information about their respective research. CMUG partners are currently involved in all of the CMIP projects and a summary of this is given in Table 2.

¹ <https://www.wcrp-climate.org/grand-challenges/grand-challenges-overview>

² <https://www.wcrp-climate.org/modelling-wgcm-mip-catalogue/modelling-wgcm-cmip6-endorsed-mips>

CMUG CCI+ Deliverable

Reference: D4.1: Exploiting CCI products in MIP experiments

Submission date: April 2021

Version: 1.3



CMUG PARTNER	MIP PROJECTS
Met Office	All MIP projects, either directly or through collaborative research with the UK institutes using the Met Office climate model The Met Office leads HighResMIP. A Met Office researcher is a panel member for CMIP6
DLR	Veronika Eyring is a panel member for CMIP6 MIPs relevant to atmospheric processes and chemistry
IPSL	LS3MIP (Land Surface, Snow and Soil Moisture Model Intercomparison Project) - the results will be valuable for the work proposed in CMUG. SPMIP for Soil Parameter MIP - the results will be particularly valuable for the work proposed in CMUG. AMIP HiResMIP (an AMIP at higher resolution)
BSC	ScenarioMIP (5x SSP2-4.5 scenario runs) DCPP VolMIP (volcpinatubo-full and volc-long-eq) HiResMIP PRIMAVERA: spinup, hist-1950, control-1950 and highres-future) AerChemMIP (piClim-2xdust) C4MIP
MPI-M	Dirk Notz is co-chair of SIMIP Researchers at MPI-M are involved in virtually all MIPs and will provide respective model output from specific simulations.
Météo France	AERCHEMMIP CFMIP DAMIP DCPP FAFMIP LS3MIP RFMIP ScenarioMIP CORDEX Plus an involvement with many others
SMHI	CMIP HighRESMIP

Table 2: Summary of CMUG involvement with CMIP projects.



4. CMUG MIP experiments with CCI products

4.1 Evaluation of modelled system memory

Lead partner: MPI-M

Author: Andreas Wernecke

Aim

The aim of this research is to develop and apply a framework that allows evaluation of the simulated memory (temporal correlation) of ECVs in a model-evaluation processing chain. It will address the following scientific question: How can we evaluate the memory of climate variables as simulated by large-scale model simulations?

Summary of Work and Results

Work on this experiment has so far focused on the Sea Surface Salinity ECV (SSS) but the general workflow is adjustable to other ECVs. The temporal auto-correlation, or memory, is an essential property of all ECVs. It describes the ability of the earth system to maintain a quantity in spite of climate variability. The memory is also closely related to the predictability of a variable and the time-frame for which data assimilation into prediction models has the potential to be beneficial. However, here we do not investigate the role of model memory in the context of (e.g. seasonal-) prediction models but for the evaluation of climate models in general. The memory of a system variable is the result of the sum of all relevant physical processes, acting on their respective time scales. A disagreement of modelled and real memory indicates either that the relevance of processes is falsely interpreted (including potentially neglecting a process completely) or that processes are misrepresented in the model so that the respective relevant time scales are wrong. Observational uncertainties can also distort the image of the real system memory where e.g. sensor white noise would reduce the observed memory.

Three statistics are used here, which are quickly introduced in the following.

The Anomaly Correlation Coefficient (ACC) is frequently used as fully localized measure of the correlation between a seasonal forecast (v) and observations (o). The ACC is the Pearson correlation coefficient for a given location and month of the year, calculated over a range of years. For the memory we treat the SSS of month x as forecast for a following month ($x+\text{lag}$). For example, the ACC can be a measure of how strongly a positive SSS anomaly in, say, January is informative for the SSS anomaly in March ($\text{lag}=2$ month), at any given location.

The lagged pattern correlation on the other hand is defined as the Pearson correlation between two time slices, calculated across all locations. The pattern correlation between January and March can therefore have different values for each year, which we average using a Fisher-Z



transformation. The pattern correlation is a global statistic describing regional memory; how long does a pattern (fingerprint) of regionally high/low anomalies persist? Limitations are the disregard towards biases (of limited concern here since the seasonal cycle/trends are not the focus area) and amplitude of the pattern. For example, if there is a spatial pattern of high/low anomalies in January which diminish homogeneously (anomalies become smaller with time but maintain their relative spatial distribution) the pattern correlation would still attest full/perfect memory.

Lagged Mean Squared Differences (MSD) (also called mean squared error) reflect a combination of change in amplitude and change in location. The MSD is easily converted into a skill score by $S_MSD = 1 - MSD / MSD_REF$, setting one to a perfect value (no differences) and zero to an MSD equal to a reference MSD. Typically reference values are based on an earlier MSD or a climatology (Section 8.3.3 in ‘Statistical Methods in the Atmospheric Sciences’; Wilks, 2019). Here we use the climatology as reference so that $S_MSD = 0$ corresponds to a lag time where the initial SSS anomaly is just as good a predictor for a later time as the climatology (i.e. zero for anomalies). Note that for lag times larger than the temporal correlation length scale (memory), the climatology is the best a-priori predictor of the SSS state, meaning that negative S_MSD are to be expected.

Here we investigate SSS memory in the CCI+ SSS product, ORAS5 reanalysis and the MPI-ESM grand ensemble (MPI-GE). We use two periods for model-to-observation comparisons which are 1979-2005 (ORAS5 and MPI-GE historical runs) and 2010-2019 (CCI and MPI-GE RCP4.5 runs). In all cases we first derive the (linearly) detrended anomalies (the respective climatologies are based on the same periods as mentioned before) and bring the MPI-GE data onto the observational (EASE-2) projection. The MPI-GE sea surface salinity extends underneath sea ice, where the view for CCI satellite observations is blocked. We use only locations for which valid SSS observations are available throughout the whole data period and use the same mask for MPI-GE data. To minimize the influence of sea ice further we limit the study area to 65° S to 65° N.

Figure 4.1.1 illustrates crucial steps towards the SSS memory analysis. The CCI+ SSS product and MPI-ESM data are brought to the same grid and masks (location of valid estimates) are synchronized (top row of Figure 4.1.1). SSS anomalies are derived year-round by subtracting the seasonal cycle and linear trends (examples for January and April 2019 shown in the second and third row of Figure 4.1.1). The anomalies (and with that the absolute SSS values) cannot be expected to agree between the data sets since they represent internal variability of the (modelled and observed) system. Again, the model runs used here are climate projections and are not intended to forecast the one realization of internal variability which the real world is taking but instead to represent plausible (alternative) realizations with realistic magnitude, spatial and temporal characteristics. The memory, represented by the ACC in the bottom row of Figure 4.1.1, is one of those characteristics which would ideally be consistent between the data sets. Overall, the ACC is considerably smaller in the CCI+ product than in the MPI-ESM and fewer locations have significant correlation. That being said, some regional similarities do exist, for example in the tropical pacific with bands of increased memory north and south of the equator as well as the north Atlantic between 10° N and 30° N and around Australia and Maritime Southeast Asia.

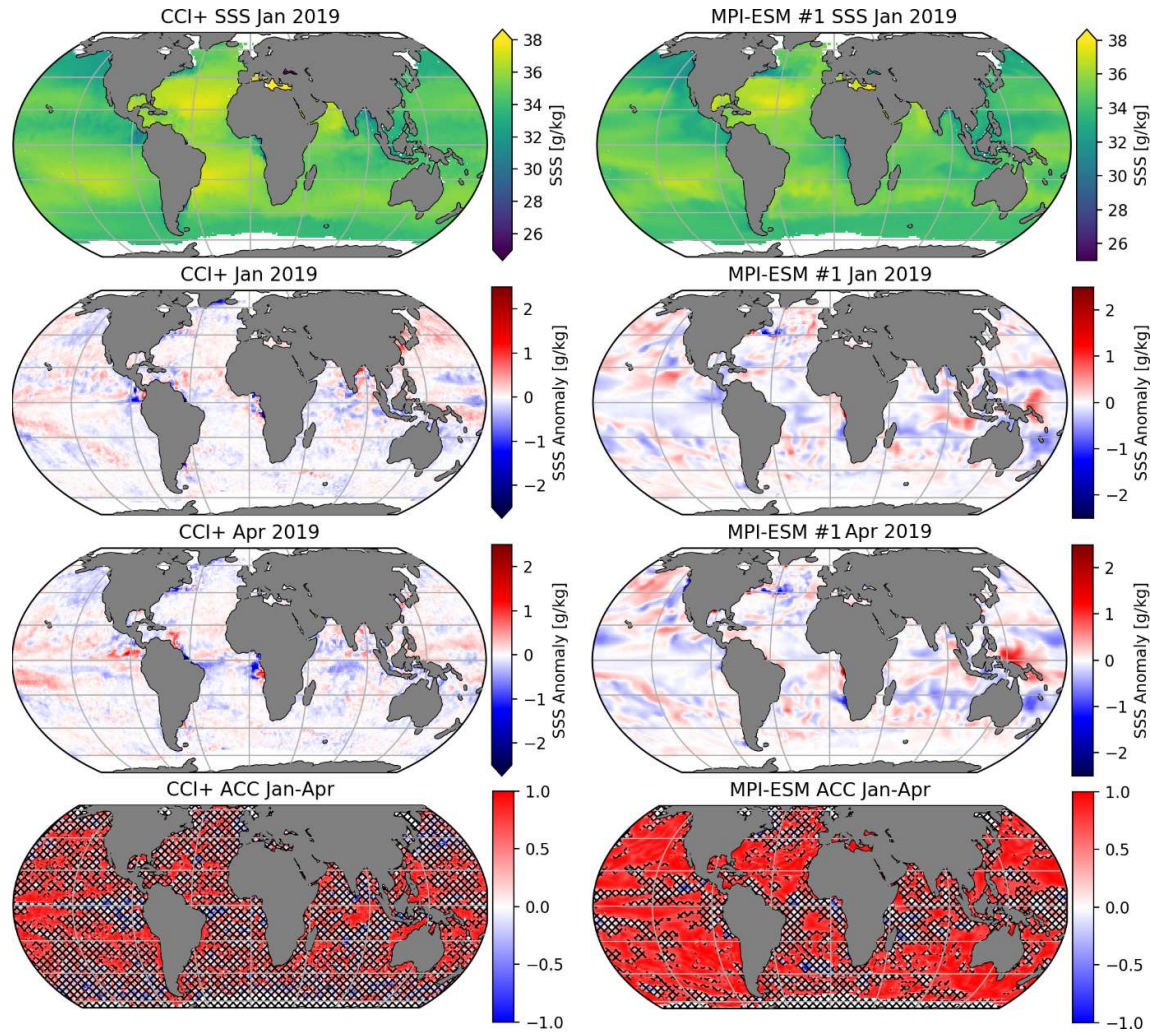


Figure 4.1.1: CCI+ satellite observations (left) and MPI-ESM grand ensemble member #1 (right) January 2019 Sea Surface Salinity (SSS) (top) and SSS anomalies for January and April 2019 (second and third row respectively) and Anomaly Correlation Coefficients (ACC, bottom row) between January and April SSS based on 2010 to 2019. Locations with ACC p -value below 0.05 (failed significance test) are hatched.

The local memory, as approached above by the ACC, can give valuable information of regional model to observation agreement. Relevant processes, leading to agreement or disagreement between the data sets, will however change throughout the year and act on a range of timescales, making a systematic investigation challenging (note that we show only the ACC between January and April as examples). The main global pattern appears to be that the observed memory is shorter than the MPI-ESM memory making local interpretations cumbersome. To test this hypothesis, we use the global anomaly pattern correlation.

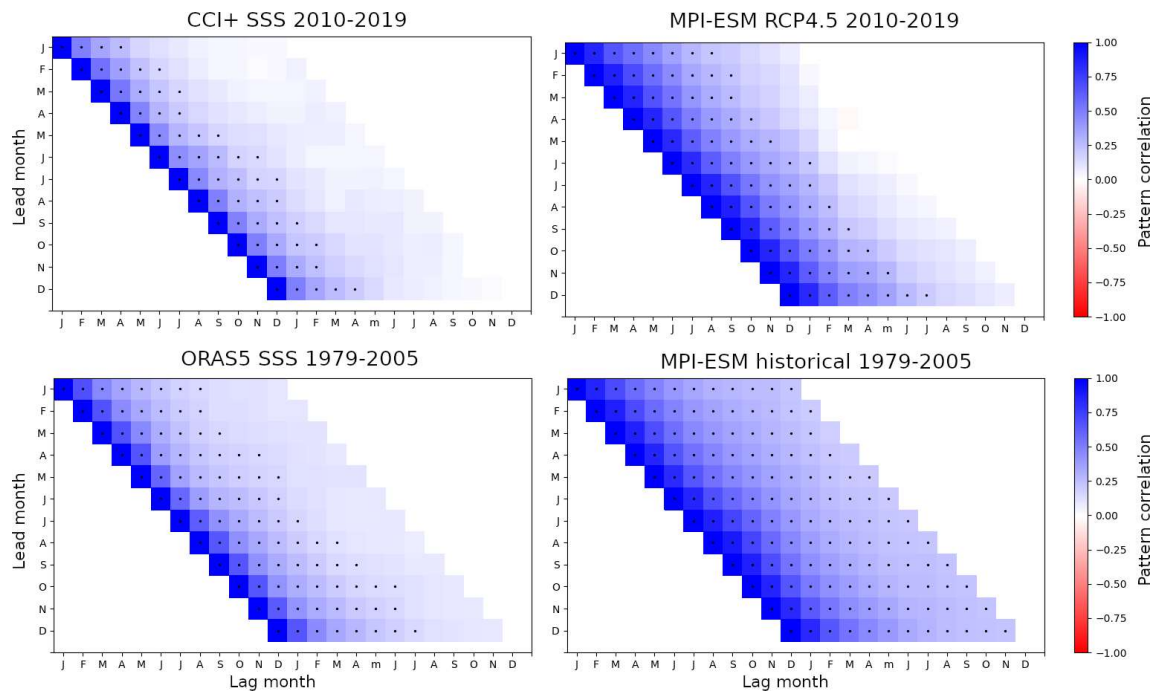


Figure 4.1.2: Global SSS anomaly pattern correlation from MPI-ESM (right) and observations (left), namely the CCI+ SSS product (top) and ORAS5 ocean reanalysis (bottom). Note that the MPI-ESM data is confined to the same time periods as the respective observations and that we use historical forcing experiment before 2005 and RCP4.5 experiment past 2005. Dots indicate significance.

We calculate the lagged pattern correlation between each month of the year (lead month) and each month of the full succeeding year (lag month). The lag period goes therefore from zero to eleven month (x-axis of Figure 4.1.2) where zero lag time corresponds to a perfect correlation of one. In general, the memory characteristics are discussed in terms of persistence (the initial short-term drop in correlation), long term memory and potential reemergence of correlations throughout the year. However, the results shown in Figure 4.1.2 do not show noteworthy variations throughout the year or any features but a monotonic drop in pattern correlation. The typical time scale of these drops differs however by data set; The CCI+ product shows the shortest memory of only about three months, followed by ORAS5 reanalysis with about five months, the ten year MPI-ESM RCP4.5 sub-period of about six to seven months and the longest memory of the 27 year MPI-ESM *historical* sub-period of more than 12 months (Figure 4.1.2).

While noise in the satellite data could result in an underestimation of the system memory, we do not expect the ORAS5 reanalysis data to be particularly noisy. The consistently longer memory in model runs compared to both types of observations therefore suggests that the MPI-ESM grand ensemble simulations have an unrealistically long modelled system memory. The temporal evolution of these model simulations is therefore apparently too smooth on short



(seasonal to yearly) time-scales. As mentioned before, the MPI-ESM RCP4.5 memory for the CCI+ period (2010-2019) is significantly shorter than for the *historical* simulations from 1979-2005. This is fully consistent with shorter memory in the CCI+ data compared to ORAS5 data which is therefore no indication for a substantial influence of noise on the CCI+ data.

The pattern correlation does not cover changes in the amplitude of the anomalies but just the relative spatial high/low anomaly distribution, which is why we complement the pattern correlation by an analysis of the MSD skill score.

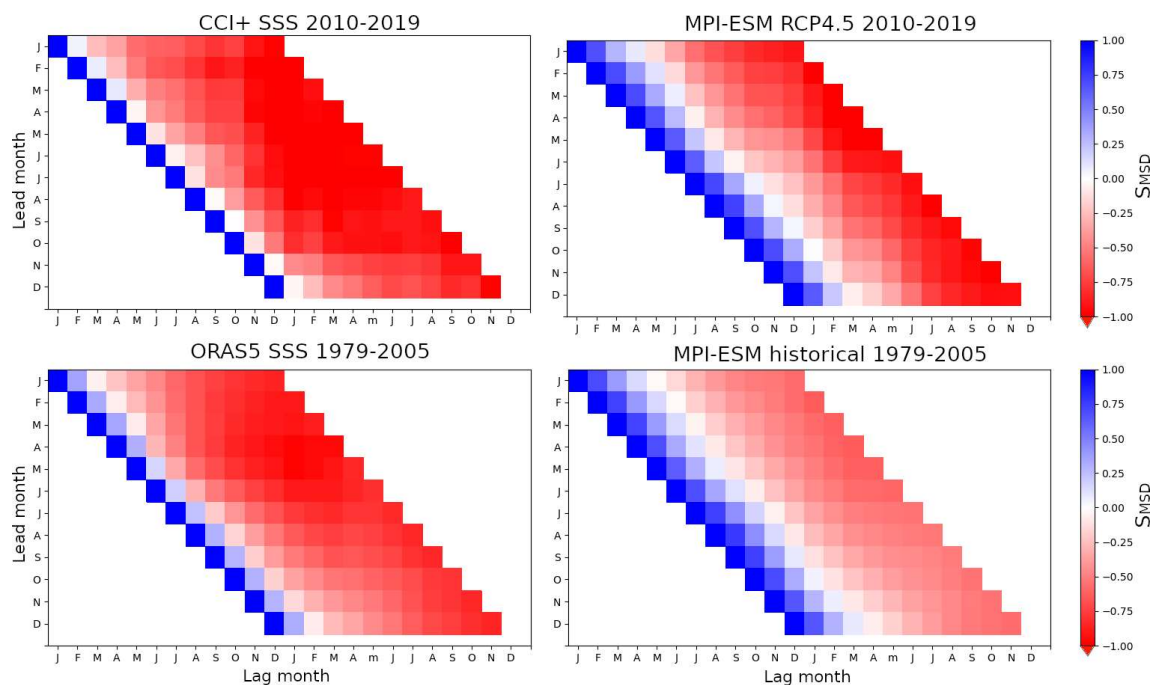


Figure 4.1.3: As Figure 4.1.2 but showing the Mean Squared Differences Skill Score (S_{MSD}) instead of the pattern correlation.

The lagged MSD Skill Score (Figure 4.1.3) shows the same behavior as the pattern correlation with the only difference that small values are reached after shorter periods which can be easily explained by the differences in the statistics. Both show a value of one for optimal agreement but while zero in the pattern correlation indicates no correlation between the two anomaly fields, an MSD Skill of zero only indicates that the MSD is as small as the climatology value. The order of length of memory by data set is the same for both statistics.

Since the memory has no clear dependency on the time of the year, as can be seen in Figure 4.1.3, we illustrate the decline of S_{MSD} as function of lag time and combine model and observational estimates in Figure 4.1.4. We further define an estimate for the memory as the first crossing of S_{MSD} with zero, i.e. the time for which the lead month can be considered a



useful, i.e. better than climatology, predictor for the lag month. Note that the absolute value of this definition of memory is strongly dependent on the statistic used (compare Figures 4.1.2 and 4.1.3) but is nevertheless useful for model to observation comparisons. It can be seen that MPI-ESM simulation can largely be separated from the observations for both data sets without consideration of seasons or any temporal averaging (Figure 4.1.4).

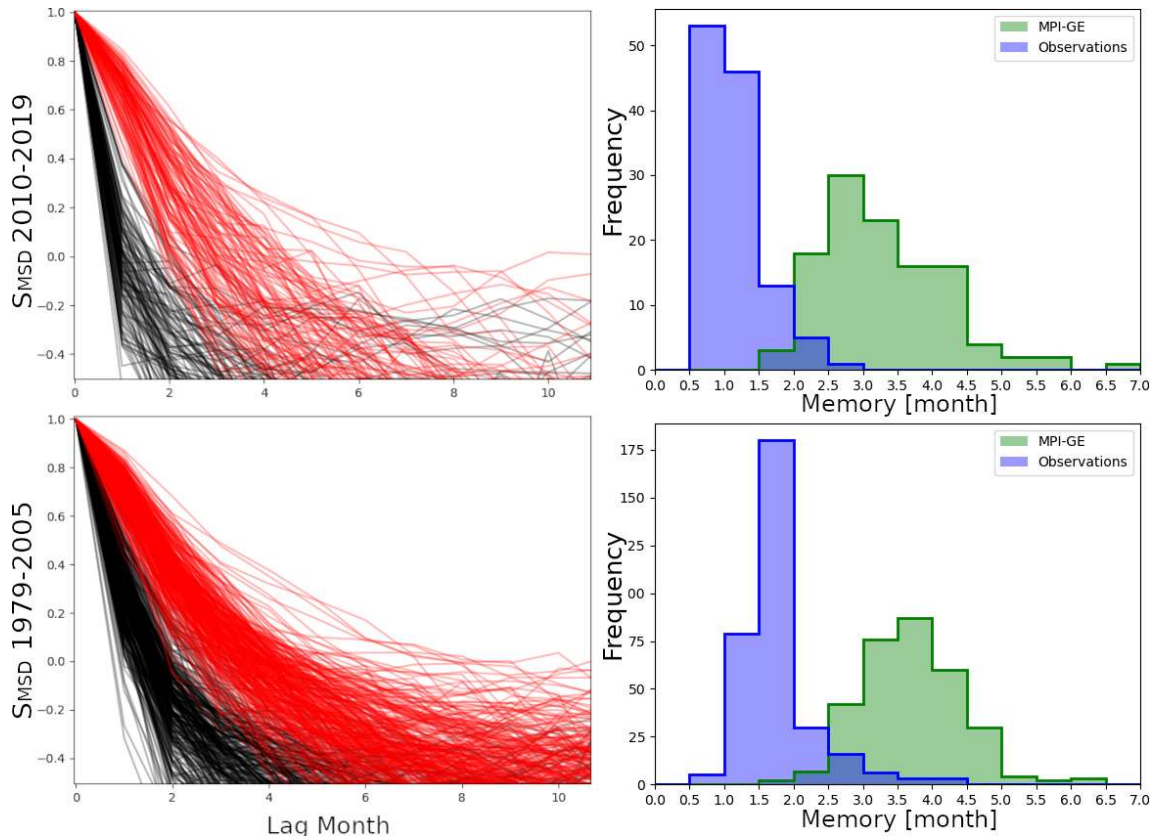


Figure 4.1.4: Decline of S_MSD with lag time for observations (black) and MPI-ESM (red) (left) where there is one line for each month of the time series, representing the decline in skill with the following month. The frequency distributions of the corresponding first crossing of S_MSD with zero using linear interpolation ('memory') is shown on the right. The CCI+ data and period are used for the top row and ORAS5 data and period for the bottom row.

Lastly, we investigate the potential of a latitudinal dependency of the memory, inspired by the findings from the ACC above. For this reason, we derive the memory (as defined above) on latitudinal bands of 15° for each month of the year. Besides the now well-established difference in absolute memory we see good agreement in the latitudinal-temporal development. The memory is largest at around $\pm 30^\circ$ N and towards 60° N with the shortest memory near the equator (Figure 4.1.5). Also the temporal development shows many similarities with a prolongation of the memory in the first half of the year (January to June) around 30° N and in



the second half of the year (July to December) at around 30° S. Small differences between observations and model are however noticeable; the tropical minimum in the MPI-ESM data lies between approximately 10° S (around June/July) to 10° N (December/January) while those points are about 5° to 10° further north and about two month earlier in both observational data sets.

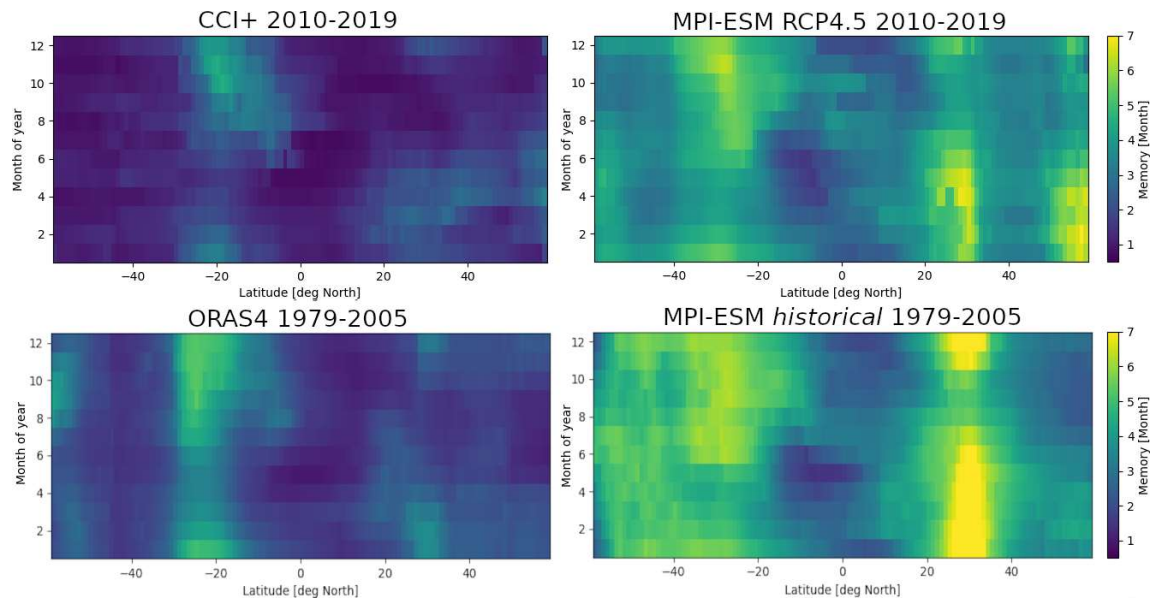


Figure 4.1.5: The memory (defined here as the first zero crossing of the MSD Skill Score) by latitude (15° bands centered at the latitudes shown) and lead month, averaged over the years and based on the data set, noted above each panel.

Publications

None so far, but we plan to describe related concrete plans in the next version of this report.

Interactions with the ECVs used in this experiment

Interactions between the CMUG and ECV projects for work on this WP in particular happened though an email exchange with the CCI+ SSS science lead where the influence of the sensor penetration depth on the characteristic depth of the surface water layer have been discussed. We concluded that under most circumstances (all but strong rain events) SSS satellite observations are representative for the surface mixed layer, which allows a one to one comparison with modelled SSS memory. The quarterly CSWG and the Integration meetings allowed for additional interactions, including with the SSS team.



Consistency between data products

So far we did not identify any inconsistencies of concern with regard to the system memory (in addition to those discussed above). There appears to be a bias in the global mean SSS between the model and observations of about 0.2 g/kg to 0.25 g/kg, which appears to be larger in the southern hemisphere than in the northern hemisphere. This biases towards MPI-ESM data are, however, consistent between reanalysis and CCI+ observations, suggesting that the model has a negative bias towards the real state.

Recommendations to the CCI ECV teams

To be completed in next version of this report.



4.2 Evaluation of model results considering observational uncertainty

Lead partner: MPI-M

Author: Andreas Wernecke

Aim

The aim of this research is to develop and apply a framework that allows one to include observational uncertainty information into a model-evaluation processing chain. It will address the following scientific question: How can we take observational uncertainty into account when evaluating large-scale model simulations?

Summary of Work and Results

So far, work in this area has focused on the sea ice ECV. When the sea ice ECV is used for model evaluation, this is in most cases done in terms of the Sea Ice Area (SIA), Sea Ice Extent (SIE) or Sea Ice Volume (SIV). Here we focus on the SIA due to known limitations of the SIE (such as resolution dependency) and it being used much more frequently than the SIV. The SIA is calculated as the Sea Ice Concentration (SIC) multiplied by corresponding pixel size, summed up over the whole hemisphere. Sometimes the difference in SIA from a few SIC products is used as a rough estimate of the SIA but with ongoing progress in SIC uncertainty quantification, an accompanying single product SIA uncertainty estimate seems overdue. The challenge is to convert local SIC uncertainty to a combined SIA uncertainty for which it is necessary to take into account the spatial covariance structure. The importance of the correlation structure for the SIA uncertainty, and with that for model evaluations, becomes clear when considering the two extremes: All SIC pixels could be considered statistically independent which would in practice result in SIA standard deviation of order 10 000 km². The other extreme is to consider all local uncertainties throughout the hemisphere as fully correlated which would increase the SIA uncertainty in practice to the order of 1 000 000 km² (based on 50 km resolution CCI+ SIC data).

Work on this WP started with the theoretical development of a spatial covariance model which combines expected correlation signatures (based on our understanding of the error sources following discussions with the CCI+ SIC team; Thomas Lavergne, Met Norway). The main challenge is to quantify covariance model parameters (of our new model or in fact any covariance model). Most prominently this is the spatial de-correlation length scale, i.e. the characteristic spatial distance at which errors in the SIC product are largely independent. We address this challenge by three different approaches, as described below.



The covariance model

The algorithmic and smearing uncertainties (as provided by the CCI+ product) are assumed to be independent, each with their own correlation matrix.

The algorithm uncertainty is expected to be largely driven by tie-point and methodological uncertainties and only to a smaller (here neglected) extent from local measurement uncertainties. Since small SIC values will be predominantly impacted by the ocean tie-point and high SIC values predominantly impacted by the 100% sea ice tie-point, we base the (hemisphere wide) algorithmic correlation solely on differences in the sea ice concentration, not on the physical distance between measurements. The following error correlation function ($c_a(x_i, x_j)$) for the algorithmic uncertainty between measurements at locations x_i and x_j , fulfills these criteria:

$$c_a(x_i, x_j) = \exp \left[\frac{-\delta_{SC}^2}{I_{SC}^2} \right]$$

where I_{SC} is a scaling parameter and δ_{SC} is the absolute difference in SIC (in percent) at the locations x_i and x_j .

The smearing uncertainty represents a range of influences on the satellite measurements related to the different footprint sizes and spillover effects from outside of the theoretical footprints. Its correlation structure is hence more complex and should fulfill the following considerations:

- The correlation should diminish with distance between locations
- Uncertainties for similar SIC values are more likely to be subject to coherent errors than across SIC gradients
- The land spillover effect near coasts is expected to cause correlated errors.

The following error correlation function for the smearing uncertainty ($c_s(x_i, x_j)$), between measurements at locations x_i and x_j , fulfills these criteria:

$$c_s(x_i, x_j) = \exp \left[\frac{-\delta_x^2}{(I_{x0} + I_{xSIC}(1 - \delta_{SIC}/100\%) + I_{xL}r_L)^2} \right]$$



with l_{x0} , l_{xSC} and l_{xL} being components of the characteristic correlation length scale, δ_x being the distance between x_i and x_j , δ_{SC} as defined before and r_L a factor representing the combined proximity to the land by:

$$r_L = \frac{l_L^2}{\delta_{L,i}\delta_{L,j}}$$

where l_L is a typical length scale for the impact of land on the correlation and $\delta_{L,i}$ being the shortest distance to land (as defined by the SIC land mask) of x_i ($\delta_{L,j}$ is defined accordingly). To restrict the maximal impact of the land spillover on the correlation we set the maximum of r_L to one. Note that l_{xL} and l_L are separate parameters, the first representing the maximal additional correlation length scale in $C_s(x_i, x_j)$ due to land influence (which can be understood as a distance the land influence is able to carry the uncertainty correlation) and the latter (l_L) representing the typical distance away from the coast which is impacted.

In summary, we defined correlation functions that match our basic expectations. It is not encompassing anti-correlations which is in line with our error characteristic expectations. The smearing error correlations diminish with distance between two measurements with the typical correlation length-scale (at which the correlation has fallen to about 0.37) between l_{x0} and $l_{x0} + l_{xSC} + l_{xL}$, depending on the sea ice concentration (longer with similar concentration values) and proximity to land (longer close to the coast). There are five free parameters (algorithmic and smearing uncertainty combined) which need to be set ($l_{x0}, l_{xSC}, l_{xL}, l_L, l_{SC}$). This is not to say that these are the only or best functional forms to represent the error correlation structure, it is one representation in line with our expectations. More research is needed to test these expectations, test other functional relationships and constrain the free parameters. The work described in the following is an early attempt to deepen our understanding in this regard.

Investigation of the CCI+ SIC error correlation

First, we derive spatial SIC correlations and SIC uncertainty correlations from repeated measurements. The rationale behind the use of the spatial SIC correlation as proxy for the SIC error correlation is that for a constant real SIC, the changes in SIC measurements would represent errors of repeated measurements. The SIC uncertainty correlation is related to the SIC error correlation by the idea that any process causing an increased uncertainty over a certain spatial footprint is more likely to cause the corresponding errors to be correlated as well. To be clear about the difference between errors and uncertainties: The uncertainty is a measure of the width of the distribution of a random variable (here the CCI SIC at a given time and location), the error is the SIC difference between a specific measurement (e.g. the SIC product value which is the center of the uncertainty distribution) and the real value. If the uncertainty estimates are good, the error distribution will be consistent with the uncertainty estimates. For example, if two locations have highly correlated uncertainties it means that if one has relatively wide probability distribution, it is very likely that the other one has a relatively wide probability



distribution as well. It does *per se* not mean that an e.g. overestimated SIC measurement at one location makes it more likely that the measurement at the other location is overestimated as well.

For Figure 4.2.1 (right) we derive the SIC correlation structure from the CCI+ SIC measurements from February 21st and use the provided uncertainties (algorithmic and smearing) from Feb. 21 2016 to receive a combined covariance estimate. This is compared (Figure 4.2.1, left) with the covariance based on our correlation model with selected parameters (here: $l_{x0} = 100\text{ km}$, $l_{xSIC} = 300\text{ km}$, $l_{xL} = 100\text{ km}$, $l_L = 100\text{ km}$, $l_{SIC} = 20\%$). The model has the advantage that, once the parameters are derived, it is available for every time and place and does adapt to changes in the ice cover dynamically. While this is just one example, it shows that sample covariance structures can show complex patterns and that the correlation model developed here is capable of representing such structures reasonably well. Note that this approach is challenging to evaluate systematically (Figure 4.2.1 shows the covariance for one day and relative to one location).

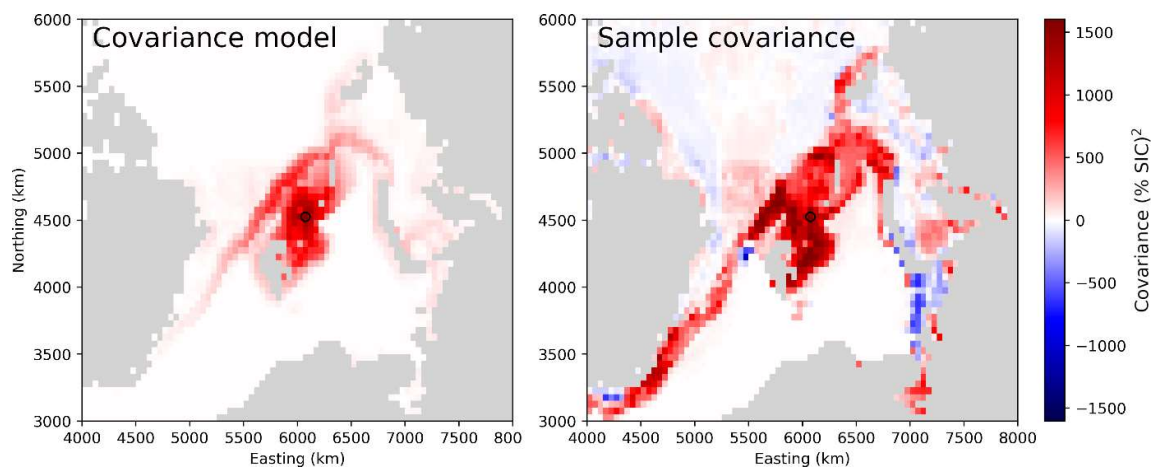


Figure 4.2.1: Spatial covariance for selected location northeast of Svalbard (black circle) from the developed covariance model on the SIC product from Feb. 21 2016 (left) and the sample SIC covariance with correlation pattern based on the years 2007 to 2016 for the same day (right).

For comparison and generalization of the previous finding we now use correlation length scales from the CCI SIC validation and inter-comparison report (PVIR) (https://icdc.cen.uni-hamburg.de/fileadmin/user_upload/ESA_Sea-Ice-ECV_Phase2_1SICCI_P2_PVIR-SIT_D4.1_Issue_1.1.pdf). These global SIC correlation length-scale estimates, kindly provided by Stefan Kern, represent the approximate circular radius of correlation in the SIC product and SIC uncertainty product. They are therefore not suited to directly constraining the parameters of our error correlation model, particularly not the non-circular components.



In the PVIR, MODIS data is used to identify regions with $\geq 90\%$ (labeled 'Pack Ice') and 0% SIC (labeled 'Ocean') and 31 day periods of the CCI product derivation from these values is used to calculate a sample correlation. The availability of MODIS SIC estimates is limited by clouds, so that this analysis is applied to windows of opportunity and represents only errors for cloud free conditions. The correlation length-scale are calculated by defining rings around the currently investigated cell and fitting an exponentially decaying function to the average correlation within each ring. This is repeated for each cell and day. The reported correlation length hence corresponds to the distance at which the correlation towards the center cell has dropped to approximately 37%

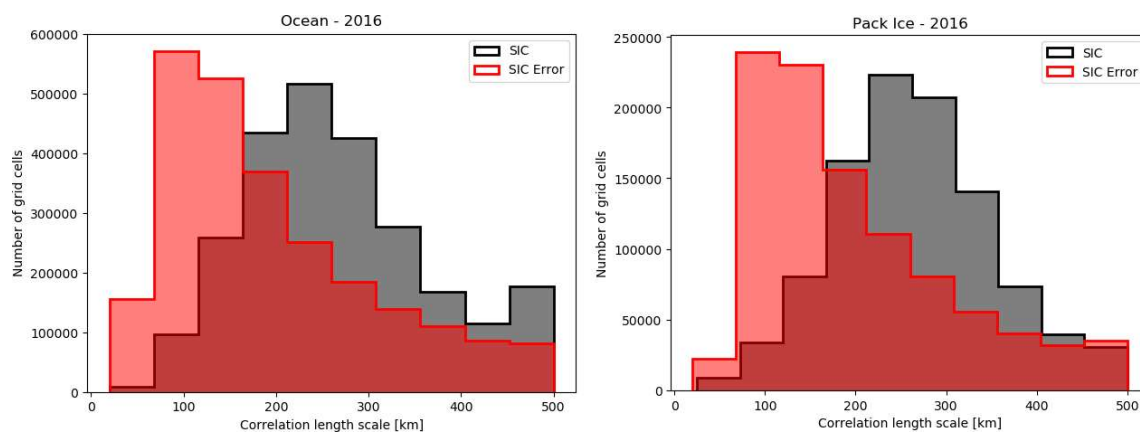


Figure 4.2.2: Frequency distributions of 2016 correlation length of the SIC and SIC uncertainty variables for preclassified open water locations (left) and pack ice locations (right). Based on calculations done for the PVIR.

In Figure 4.2.2 we see the distribution of correlation length scales for the whole Arctic basin within year 2016. Other years and quarterly assessments show very similar results (not shown). The differences in SIC error correlation length scales between pack ice and ocean conditions are very small (compare left and right of Figure 4.2.2). This is a promising result since it means that there are no indications for a dependency on the correlation length on the SIC values or between typical pack ice and ocean regions. This provides no information about a potential dependency on SIC gradient. The SIC uncertainty product has shorter correlation scales than the SIC product (red vs. black histograms). The range of values is mostly between one hundred to a few hundred kilometers.

Lastly we approach the error correlation by triangulation of independent satellite SIC products. This approach avoids any assumptions about the real state of the SIC (y) since it is the same for all SIC products and cancels out when basing the calculations solely on the differences in SIC products. Figure 4.2.3 illustrate this approach and provides the derived equations which assume that the unbiased SIC product errors (e_1 to e_3) are independent between the products. This assumption might not be justified, considering similarities in used satellite sensors, frequency bands and retrieval approaches.



For Figure 4.2.4 we use daily SIC fields from all days in February (excluding the 29.th) for the years of 2003 to 2017 (excluding 2012 and parts of Feb. 2016 due to missing data). It is based on the CCI+ SIC, NASA team algorithm (as provided by NSIDC, doi: <https://doi.org/10.7265/N59P2ZTG>) and SSMI/ASI algorithm (as provided by the ICDC <https://icdc.cen.uni-hamburg.de/seaiceconcentration-asi-ssmi.html>). Here we can combine several years of February data due to reduced dependence of the real state of the sea ice for this approach.

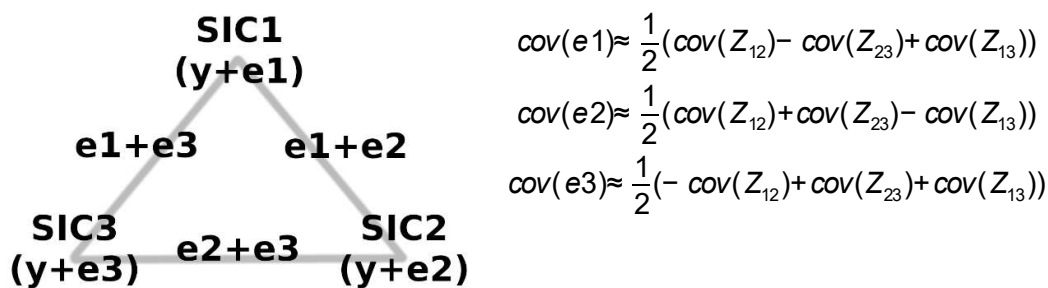


Figure 4.2.3: Schematic of SIC error triangulation and corresponding derived equations with y representing the real SIC, e_i being the error of SIC product i and Z_{ij} being the difference in SIC product i and j .

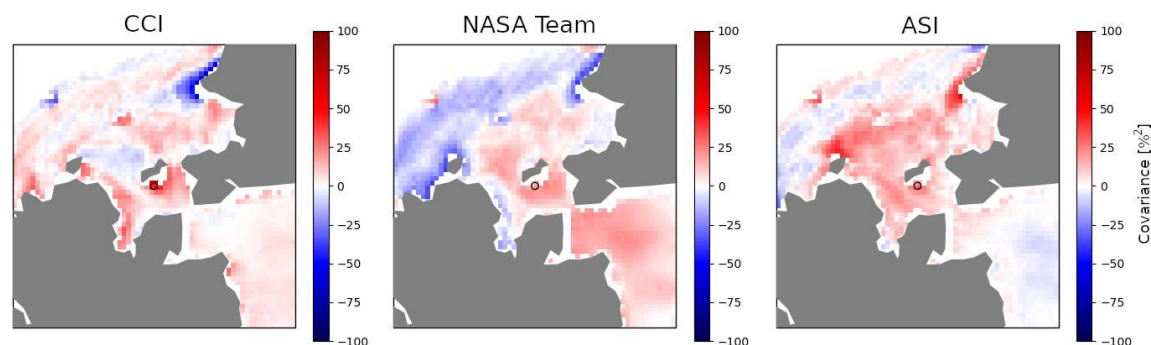


Figure 4.2.4: Covariance estimates (equations given in Figure 4.2.3) for February (as example) of three SIC products (left: CCI+, center: NASA team, right: SSMI ASI) relative to the location marked by a black circle, approx. 200 km south of the Bering strait and just north of St. Lawrence Island.

The covariance estimates in Figure 4.2.4 show some differences between the products. The NASA team and ASI products have larger correlation length scales of about 400 km in radius (the shown box covers an area of 1600 km \times 1600 km) where the CCI covariance seems to be



more localized. The NASA team product has a stronger connection across the Bering Strait than the ASI product and shows in addition lower covariance along the coasts.

A major question is how reliable these estimates are; the assumption of independent errors of the products might not hold. To investigate the robustness of our approach we use a fourth SIC product (the Bootstrap Algorithm from the NSIDC doi: <https://doi.org/10.7265/N59P2ZTG>) and repeat the above analysis with each possible pair of three. We investigate the dependency of the CCI+ SIC product error covariance estimate on the choice of the two other products which are used to derive it. Ideally all three covariance estimates in Figure 4.2.5 would be in good agreement. While there are some consistent features (e.g. reduced CCI+ covariance across the Bering strait and mostly increased covariance near the coast), there are also substantial differences (Figure 4.2.5). This is thought to be caused by a failure of the independence assumption between the SIC products. We derived error covariance estimates for all four products and analyzed other locations and seasons and find that this approach appears to be more suited for the NASA Team and ASI algorithms (higher consistency, not shown). There are two likely reasons for this. (1) CCI+ error correlations are typically weaker which makes it more likely that weaknesses in these estimates are overpowering the signal and/or (2) the cross-product error correlations are in such a way that they do have a stronger impact the CCI+ product (which is not a quality characteristic). In the equations, allowing for a positive cross-product error correlation for two of the three involved SIC products results in an underestimation in the spatial error covariance estimates of the two correlated products and an overestimation of the spatial covariance of the third, independent SIC product.

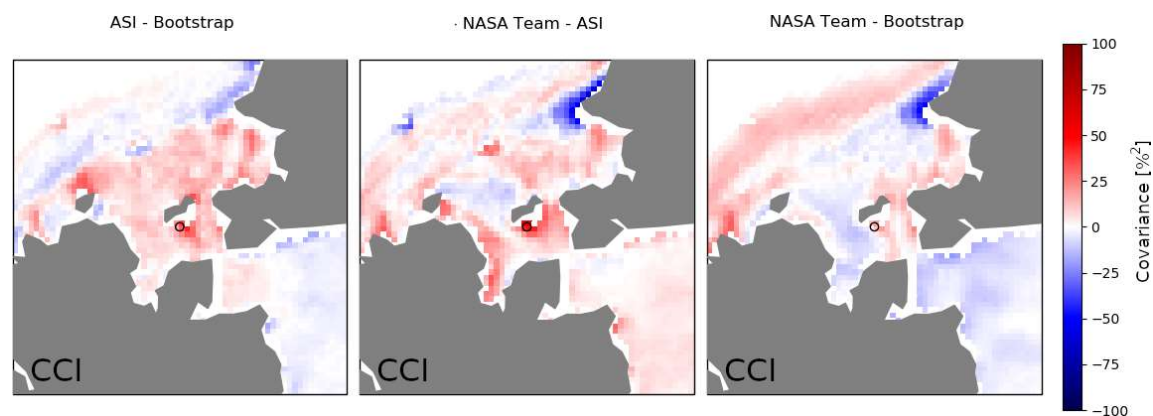


Figure 4.2.5: Covariance estimates (equations given in Figure 4.2.3) for February of the CCI+ SIC product based on triangulation with three sets of other SIC products (left: SSMI/ASI + Bootstrap, center: NASA team + SSMI/ASI, right: NASA Team + Bootstrap) relative to the location marked by a black circle, approx. 200 km south of the Bering strait and just north of St. Lawrence Island.



Synthesis

We developed an SIC error correlation model and attempted to constrain the corresponding parameters based on a statistical analysis of the data. None of the approaches (individual SIC sample correlations, re-analysis of the PVIR circular correlation estimates and a triangulation of error correlations by a combination of several SIC products) lead to a robust estimate of the model parameters. It did, however allow us to improve our understanding of the SIC error characteristics and cross-product correlations. Overall, spatial covariance structures can have significant non-circular components (Figure 4.2.1), correlation length scales are rarely below 100 km and frequently reach several hundred km (Figure 4.2.2, Figure 4.2.5), and there are weak indications for increased covariance pattern in the CCI+ products near land (Figure 4.2.5, center and right). Our correlation model is capable of incorporating all those findings. The lower bound of correlation length (l_{x0}) should be chosen to be no less than 100 km and the sum of the two additional length scales (l_{xl} and l_{xlc}) should be at least a few hundred km to cover the whole range of found SIC error correlation length scales (Figures 4.2.1, 4.2.2 and 4.2.5). If simple circular error correlation models are used we would suggest a few hundred kilometers as length scale. Note that neglecting the error correlation when e.g. deriving the SIA uncertainty would result in an implicit decision to set the characteristic error correlation length scale to a value well below the SIC product resolution (zero), which would in general not be in agreement with our results.

Publications

None so far, but we plan to describe related concrete plans in the next version of this report.

Interactions with the ECVs used in this experiment

Interactions between the CMUG and ECV projects for work on this WP in particular happened through an email exchange with CCI+ SI team members (Thomas Lavergne, Stefan Hendricks and Stefan Kern) as well as joining and presenting at meetings, including CCI+ colocation meetings and the CCI+ SI progress monitoring meeting in March 2021.

Consistency between data products

This section will provide a record of any inconsistencies found between ECV products, and will be completed in the next version of this report.

CMUG CCI+ Deliverable

Reference: D4.1: Exploiting CCI products in MIP experiments

Submission date: April 2021

Version: 1.3



Recommendations to the CCI ECV teams

To be completed in next version of this report.



4.3 Evaluation of model results considering the abstraction level of observational products

Lead partner: MPI-M

Author: Dirk Olonscheck

Aim

The aim of this research is to develop and apply a framework that allows one to estimate the ideal abstraction level at which a model evaluation should be carried out. It will address the following scientific question: At which observational abstraction level should we evaluate large-scale model simulations?

Summary of Work and Results

To be completed in next version of this report.

Publications

None so far, but the interest in the results leading to a journal or conference publication will be described in the next version of this report.

Interactions with the ECVs used in this experiment

In the first 12 months of this phase of CMUG work there have been interactions with the SSS, Snow, SST, SI and LST CCI ECV projects at the quarterly CSWG meetings and the Integration meetings. Contact outside that has been only to check on the continuation of the SI and SST projects, and to learn about the beta data that LST announced was available in late 2019. Interactions with the SIMIP project are planned for the future.

Consistency between data products

This section will provide a record of any inconsistencies found between ECV products, and will be completed in the next version of this report.

Recommendations to the CCI ECV teams

To be completed in next version of this report.



4.4 Optimal spatial and temporal scales for model evaluation

Lead partner: MPI-M

Authors: Dirk Olonscheck

Aim

The aim of this research is to develop and apply a framework that allows one to estimate the ideal spatial and temporal time horizon at which a model evaluation should be carried out to minimize the impact of observational uncertainty. It will address the following scientific question: At which time and space scale should we evaluate large-scale model simulations?

Summary of Work and Results

To be completed in next version of this report.

Publications

None so far, but the interest in the results leading to a journal or conference publication will be described in the next version of this report.

Interactions with the ECVs used in this experiment

In the first 12 months of this phase of CMUG work there have been interactions with the SSSal, Snow, SST, SI and LST CCI ECV projects at the quarterly CSWG meetings and the Integration meetings. Contact outside that has been only to check on the continuation of the SI and SST projects, and to learn about the beta data that LST announced was available in late 2019. Interactions with the SIMIP project are planned for the future.

Consistency between data products

This section will provide a record of any inconsistencies found between ECV products, and will be completed in the next version of this report.

Recommendations to the CCI ECV teams

To be completed in next version of this report.



4.5 Evaluation of model results considering internal variability

Lead partner: MPI-M

Authors: Dirk Olonscheck, Dirk Notz

Aim

The aim of this research is to develop and apply a framework that allows one to consider the impact of internal variability into a model-evaluation processing chain. It will address the following scientific question: How can we take internal variability into account when evaluating large-scale model simulations?

Summary of Work and Results

The work done in the first year of this CMUG research period (October 2018 to September 2019) was on the methodology that will be used on the new CCI+ datasets when they are available. The method allows one to easily take model-specific internal variability into account when evaluating simulations from global climate models. This lays the methodological basis for taking internal climate variability into account when evaluating climate-model simulations with the forthcoming CCI+ ECVs. The background research on which the CMUG work is based was published in Olonscheck and Notz, 2017, and an evaluation using CMIP5 simulations from that paper is shown in Fig. 4.5.1.

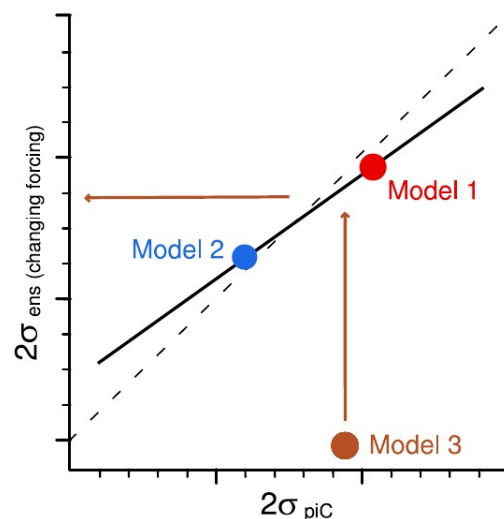


Figure 4.5.1:
Schematic view of the method for estimating internal variability for different forcing scenarios.



The basic version of the method regresses the estimate of internal variability derived from the preindustrial control simulation of a model (x axis) on the ensemble standard deviation of models with ensemble simulations such as models 1 and 2 (y axis). The unity line as a reference is indicated by the dashed black line. For the extended version, a constructed ensemble standard deviation can be derived for models with a single simulation (model 3) using the regression line through models 1 and 2. The extended version requires a consistent response of the models with ensemble simulations. A summary of the scientific outcomes of the research are:

1. Development of a new method that allows us to consistently estimate internal climate variability and its change over time for all models within a multimodel ensemble such as CMIP5 by regressing each model's estimate of internal variability from the preindustrial control simulation on the variability derived from a model's ensemble simulations.
2. We find a highly variable model-specific internal variability of sea-ice volume and sea-ice area.
3. The method allows for the evaluation of climate-model simulations by uniformly taking model-specific internal variability for all models into account.

Publications

None so far, but the interest in the results leading to a journal or conference publication will be described in the next version of this report.

Interactions with the ECVs used in this experiment

In the first 12 months of this phase of CMUG work there have been interactions with the SSSal, Snow, SST, SI and LST CCI ECV projects at the quarterly CSWG meetings and the Integration meetings. Contact outside that has been only to check on the continuation of the SI and SST projects, and to learn about the beta data that LST announced was available in late 2019. Interactions with the SIMIP project are planned for the future.

Consistency between data products

This section will provide a record of any inconsistencies found between ECV products, and will be completed in the next version of this report.

Recommendations to the CCI ECV teams

To be completed in next version of this report.



4.6 Evaluation of model results considering a combination of sources of uncertainties

Lead partner: MPI-M

Authors: Dirk Olonscheck, Dirk Notz

Aim

The aim of this research is to develop and apply a framework that allows one to include both observational uncertainty and uncertainty arising from internal variability into a model-evaluation processing chain. It will address the following scientific question: How can we take observational uncertainty and internal variability into account when evaluating large-scale model simulations?

Summary of Work and Results

The work done in the first year of this CMUG research period (October 2018 to September 2019) was on the methodology that will be used on the new CCI+ datasets when they are available. The introduced plausibility variable (below) allows one to take both model-specific internal variability and observational uncertainty into account for evaluating climate-model simulations. We did so to evaluate the CMIP5 climate-model simulations as shown in Fig. 4.6.1. This comprehensive evaluation approach will be applied to comparing climate-model simulations with the CCI+ ECVs. The background research on which the CMUG work is based was published in Olonscheck and Notz (2017).

We introduce a plausibility variable as a measure of model fidelity, which takes both the model-specific internal variability (σ_{mod}) and the observational or reanalysis uncertainty (δ_{ref}) into account:

$$\phi = \frac{\overline{\text{mod}} - \overline{\text{ref}}}{\sqrt{\sigma_{\text{mod}}^2 + \delta_{\text{ref}}^2}}$$

This approach to evaluate climate-model simulations considers both internal variability and observational uncertainty and thus links to Task 4.2.



The results allow for a distinction between model deviations that are plausible due to internal variability and reference-data uncertainty and those that cannot be explained by these sources of uncertainty, pointing to model biases.

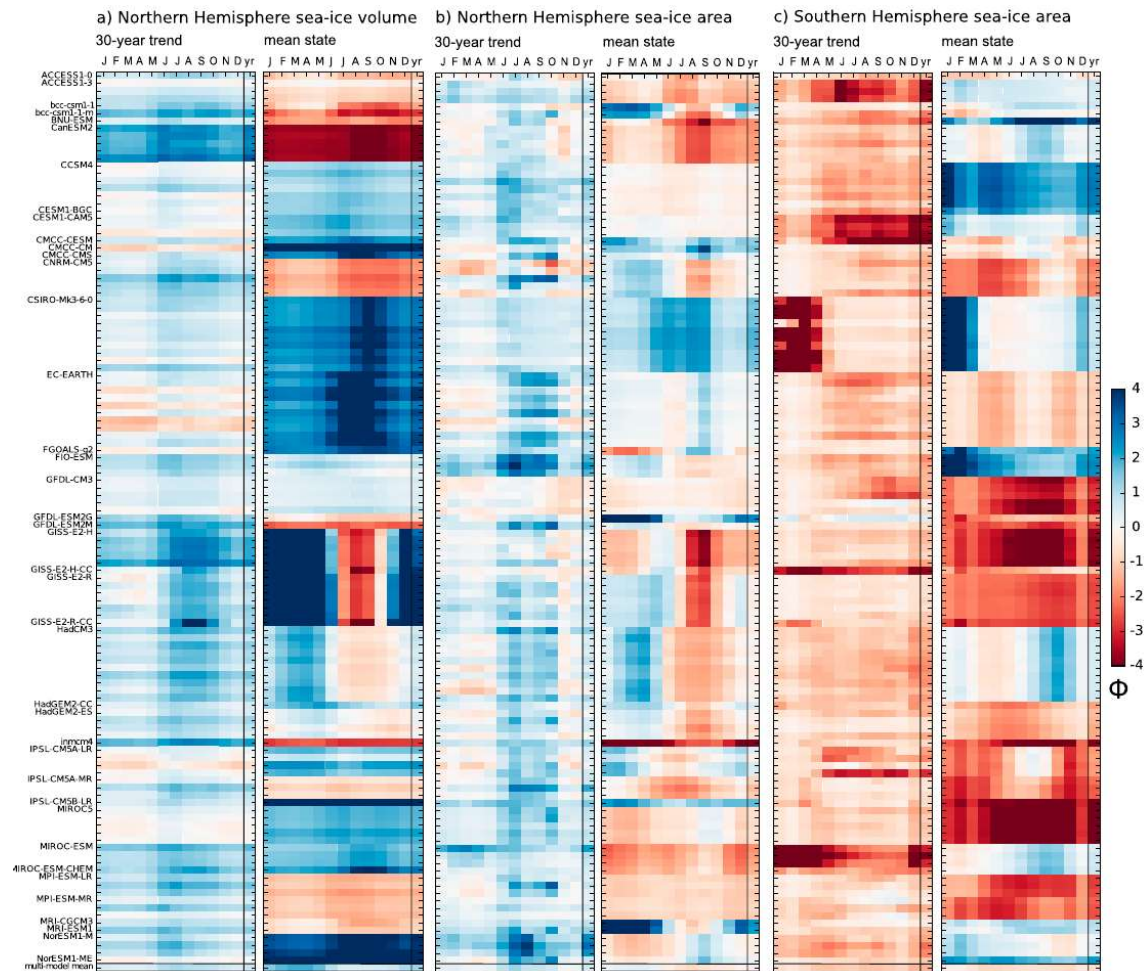


Figure 4.6.1: Portrait plot of the plausibility of CMIP5 sea-ice simulations for the 30-yr trend and the mean state of (a) Northern Hemisphere sea-ice volume, (b) Northern Hemisphere sea-ice area, and (c) Southern Hemisphere sea-ice area based on the distance between each extended historical CMIP5 model simulation and reference data (PIOMAS for Northern Hemisphere sea-ice volume and satellite sea ice data from a CCI precursor dataset, Meier 2013, for sea-ice area). Deviations are shown in units of “phi”, which combines Δ_{ref} and σ_{mod} ; a model’s negative (red) and positive (blue) deviation with respect to reference data are indicated. Note that each model name is attached to the first ensemble simulation only.



Publications

None so far, but the interest in the results leading to a journal or conference publication will be described in the next version of this report.

Interactions with the ECVs used in this experiment

In the first 12 months of this phase of CMUG work there have been interactions with the SSSal, Snow, SST, SI and LST CCI ECV projects at the quarterly CSWG meetings and the Integration meetings. Contact outside that has been only to check on the continuation of the SI and SST projects, and to learn about the beta data that LST announced was available in late 2019. Interactions with the SIMIP project are planned for the future.

Consistency between data products

This section will provide a record of any inconsistencies found between ECV products, and will be completed in the next version of this report.

Recommendations to the CCI ECV teams

To be completed in next version of this report.



4.7 Skill assessment of the DCPD decadal predictions

Lead partner: BSC

Authors: Roberto Bilbao, Louis-Philippe Caron.

Aim

The aim of this research is to produce an extensive model skill assessment of the decadal hindcasts done within DCPD (Decadal Climate Prediction Project, Boer *et al.* 2016; and thus contributing to CMIP6 initiative) the longest CCI products as an independent source for validation, thus testing at the same time the consistency of CCI data with the reference datasets used for their initialization. It will address the following scientific questions:

1. Which are the regions/variables with more skill for decadal prediction across climate models?
2. Can CCI/CCI+ data help to identify if these are robust across datasets?
3. Does skill arise for different variables over the same region?
4. Can this help to identify the processes behind the skill?

Summary of Work and Results

A preliminary analysis of the skill over the whole period covered by DCPD has been done, evaluated against non-ESA products. (ESA products cover a shorter period and will be included in the following reporting period, to wait for longer or better products to become available).

The BSC recently completed (Sept 2019) the CMIP6 decadal hindcasts using the EC-Earth coupled global climate model (<https://www.ec-earth.org>), to contribute to the Decadal Climate Prediction Project (DCPD) component A of the World Climate Research Center (WCRP). This forecast system consists in 10-member ensembles of 11 year-long hindcasts initialized each year on 1st November between 1960 to 2016. The decadal predictions are performed with a resolution of T255L91 in the atmosphere and 1° and 75 vertical levels in the ocean. The initialization technique used is full-field initialisation. Atmospheric initial conditions are generated using ERA-40 and ERA-Interim. Land initial conditions are part of ERA-40 prior to 1979. From then onwards ERA-Land is corrected with GPCP observations and used as land initialisation. Ocean and sea-ice initial conditions have been produced using a NEMO-only simulation forced by DFS5.2 atmospheric fields and nudged towards ORAS4.



A preliminary analysis of skill in the EC-Earth hindcasts has been carried out for monthly-mean global-mean sea surface temperature (SST) (Figure 4.7.1a) and several climate variability indices derived from SST: the Atlantic Multidecadal Variability (AMV) index (Figure 4.7.1c) calculated with the Trenberth and Shea (2006) definition, and El Niño Southern Oscillation (ENSO) index (Figure 4.7.1e) defined as the SST average over the Nino3.4 box (5S-5N and 170-120W). Beforehand, hindcast anomalies have been computed with respect to the period 1970-2005 using a lead-time dependent climatology. To quantify the deterministic skill the anomaly correlation coefficient (ACC) has been used (Figure 4.7.1). For this preliminary analysis three observational products have been used as a reference: ORAS4, EN4 and HadISST.

The ACC of global-mean SST in EC-Earth hindcasts shows high skill for the 5 forecast years (Figure 4.7.1b). A large part of the skill of the decadal predictions is associated with the global warming trend, thus next steps will compare the decadal hindcast (DCPP) will be compared with the non-initialized CMIP6 historical simulations (DECK+ScenarioMIP) to determine the impact of the initialization. Figure 4.7.1d shows that the model has high skill in reproducing the AMV. For ENSO the model is capable of skillfully reproducing the observations for the first few months but the skill drops to zero by the second year.

Since BSC recently finished the DCPD simulations, the future plan is to continue the verification analysis of ECVs focused on the biases and skill, both deterministic (e.g. ACC, RMSSS and MSSS) and probabilistic (e.g. RPSS). In this preliminary analysis of SST (and SST derived indices) we did not use CCI/CCI+ data since the objective was to verify the entire hindcast period (1960-2015), however we will also verify the shorter period covered by CCI/CCI+ data for comparison, putting a special emphasis in determining if the skilful regions are robust. The skill assessment will also include level and cloud cover, two of the longest CCI records available.

For decadal hindcast verification it is ideal to have the longest observational records possible to most accurately and robustly assess the skill of the prediction system. Since the climate model spatial and temporal resolution of the DCPD simulations is about 1° and monthly mean respectively, it would be useful for this analysis to put the emphasis in the design of Level 3 products (gridded) on maximising the length of the record (preferably 30yrs long) and no need for higher temporal resolution than monthly, even at the expense of the quality of the data.

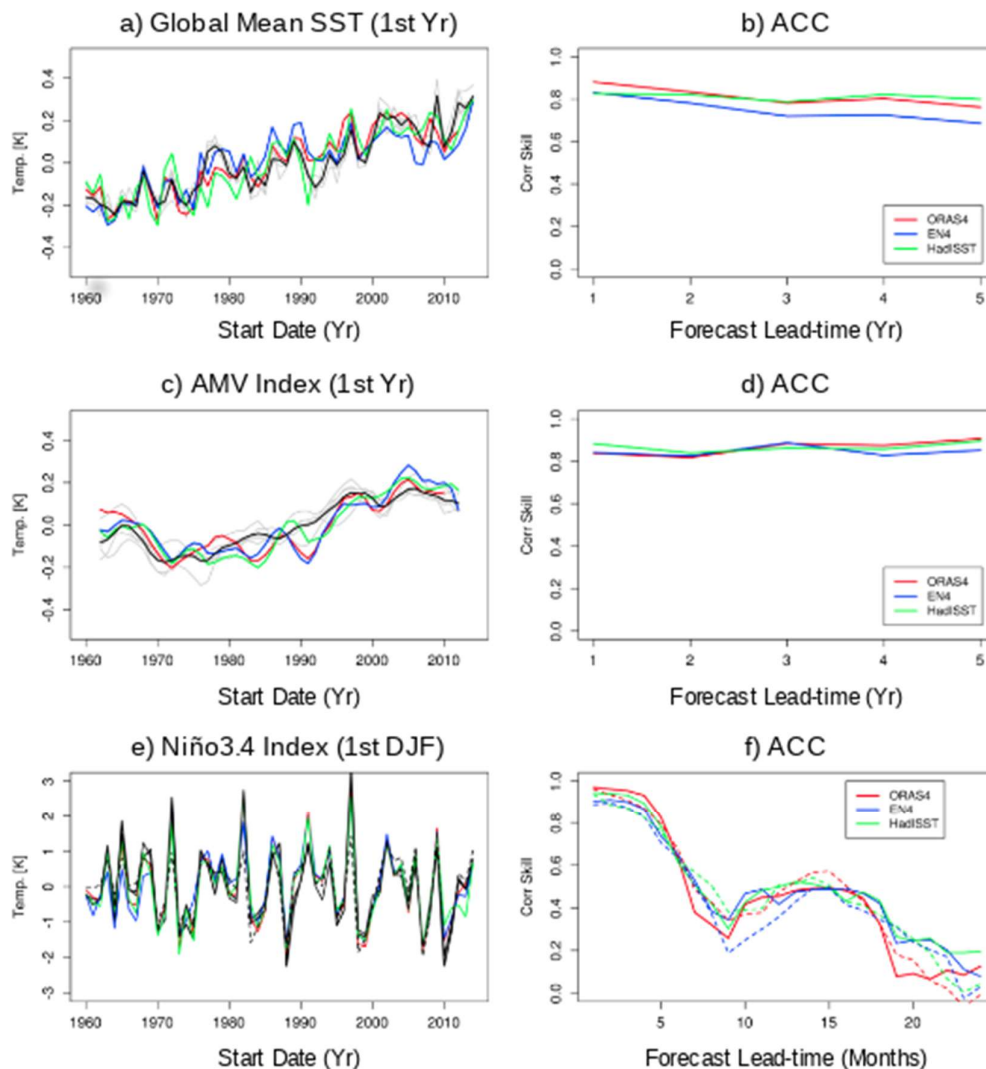


Figure 4.7.1. a) Annual-mean global mean SST for forecast lead time year 1 for the ensemble mean decadal predictions (black), individual members (grey) and three observational product: ORAS4 (red), EN4 (blue) and HadISST (green)). b) Anomaly correlation coefficient (ACC) of the ensemble mean hindcasts and observations. c) As figure a) but for the AMV (Trenberth and Shea, 2006 definition). d) ACC of the AMV. e) As figure a) for the Niño3.4 index for the first DJF. f) ACC of the Niño3.4 index.

Publications

None so far, but the interest in the results leading to a journal or conference publication will be described in the next version of this report.



Interactions with the ECVs used in this experiment

In the first 12 months of this phase of CMUG work there have been interactions with the Sea Level, SST, and Clouds CCI ECV projects at the quarterly CSWG meetings and the Integration meetings. Contact outside that has been only to learn about the continuation datasets they will be producing in CCI+. Further interactions with the ScenarioMIP and Decadal Climate Prediction projects are planned for 2020.

Consistency between data products

This section will provide a record of any inconsistencies found between ECV products, and will be completed in the next version of this report.

Recommendations to the CCI ECV teams

To be completed in next version of this report.



4.8 Use LST products to develop and test simple models relating the LST versus air temperature (near surface) difference to vegetation moisture stress

Lead partner: Met Office

Authors: Rob King

Aim

The aims of this research are to: 1) use the differences between LST and Temperature (near surface) to assess spatial and temporal variations in vegetation moisture stress across biomes. SM will also be used to examine the vegetation moisture stress. The biomes will be characterised by AGBiomass and LC. 2) Understand relationships between LST and Temperature in the context of vegetation carbon exchanges across biomes and regions. 3) Assess the potential for using LST versus Temperature relationships as a large-scale monitor of vegetation moisture stress. It will address the following scientific questions:

1. Can LST versus Temperature relationships be used to monitor large-scale vegetation moisture stress across different biomes and regions?
2. What quality information can be learned from the ancillary ECVs used in this study?

Key features

1. Understand how LST to (near surface) air temperature differences vary across biomes and to different biomes.
2. Understand how vegetation moisture stress effects LST to (near surface) air temperature differences to give indicators of moisture stress for particular biomes.

Summary of Work and Results

We have carried out some preliminary investigations and familiarisation with the soil moisture CCI data that is currently available and have started looking at the beta CCI LST data that has just become available.



Publications

None so far, but the interest in the results leading to a journal or conference publication will be described in the next version of this report.

Interactions with the ECVs used in this experiment

In the first 12 months of this phase of CMUG work there have been interactions with the LST, AGB, SM and LC CCI ECV projects at the quarterly CSWG meetings and the Integration meetings. Contact outside that has been with LST who have already produced a beta dataset, and AGB (by email) to discuss data specifications and access, and the wider question of coordinated work on using the AGB data in a land surface climate model. Interactions with SM and LC have been to learn about the continuation datasets they will be producing in CCI+. Interactions with the LUMIP and Decadal Climate Prediction projects are planned for 2020.

Consistency between data products

This section will provide a record of any inconsistencies found between ECV products, and will be completed in the next version of this report.

Recommendations to the CCI ECV teams

To be completed in next version of this report.



4.9 Use CCI+ products and simple models developed in WP4.8 to evaluate performance of modelled LST versus air temperature, using multiple up-to-date land surface and Earth System models

Lead partner: Met Office

Authors: Rob King

Aim

The aim of this research is to evaluate how well the observed relationships between LST and Temperature across different vegetation types and moisture regimes are captured by the JULES land surface model, UKESM1 and other CMIP5 and 6 (where available) Earth System Models. It will address the following scientific question:

1. Can models capture the LST versus Temperature (near surface) relationships observed with satellite products across different vegetation types and moisture regimes?

Key features

1. Identify biome specific relationships between LST and near-surface air temperatures in LST CCI data
2. Evaluate the models (listed above) in their LST and air temperature, to understand how they capture the relationship seen in the CCI data. This evaluation will cover different biomes to capture both differing vegetation types (land cover) and (soil) moisture regimes.

Summary of Work and Results

We have some insights from a preliminary investigation about the behaviour of JULES in particular biomes when skin temperatures (LST) are compared with the driving air temperatures.



Publications

None so far, but a paper on the evaluation of modelled seasonality in vegetation is planned.

Interactions with the ECVs used in this experiment

In the first 12 months of this phase of CMUG work there have been interactions with the LST, AGB, SM and LC CCI ECV projects at the quarterly CSWG meetings and the Integration meetings. Contact outside that has been with LST who have already produced a beta dataset, and AGB (by email) to discuss data specifications and access, and the wider question of coordinated work on using the AGB data in a land surface climate model. Interactions with SM and LC have been to learn about the continuation datasets they will be producing in CCI+. Interactions with the LS3MIP, C4MIP, LUMIP and Decadal Climate Prediction projects are planned for 2020.

Consistency between data products

This section will provide a record of any inconsistencies found between ECV products, and will be completed in the next version of this report.

Recommendations to the CCI ECV teams

To be completed in next version of this report.



4.10 Comparison of CCI products for studying vegetation variations with other satellite products and land surface models

Lead partner: Met Office

Authors: Rob King

Aim

The aims of this research are to: 1) Compare the seasonal timing and magnitude of vegetation-relevant CCI products with other satellite products (including MODIS) and vegetation variables from existing historic model runs (of JULES, UKESM1, CMIP5/6). 2) Identify significant differences in the timing, location and vegetation types between CCI products and other satellite and model data. 3) Suggest key areas for model development to improve vegetation seasonality. 4) Contribute results to a multi-model evaluation conducted in the CRESCENDO project. It will address the following scientific question:

1. Can the large-scale CCI ECV satellite products be used to improve representation of sensitivities and thresholds between vegetation productivity (and other carbon cycle processes) and climate in land surface/Earth System Models?

Key features

- Evaluate modelled vegetation phenology (seasonal timing and magnitude) for JULES UKESM1 and CMIP5/6 historic runs using CCI (and other e.g. MODIS) vegetation products.
- Contribute to multi-model ensemble evaluation for CRESCENDO project.

Summary of Work and Results

Preliminary evaluation of vegetation phenology peak of season modelled with CRESCENDO project models has been conducted using Leaf Area Index monthly products from MODIS and Copernicus Global Land Surface (GLS). Results show significant differences (up to 5) in the magnitude, and variations (of 1-3 months) in the timing of peak LAI between models. Models showed generally later peaks in LAI than the MODIS and GLS satellite products, which were consistent with each other. Other vegetation variables, including Biomass CCI, will be used to assess the magnitude and timing of peak productivity. Initial contact has been made with the

CMUG CCI+ Deliverable

Reference: D4.1: Exploiting CCI products in MIP experiments

Submission date: April 2021

Version: 1.3



Biomass CCI project lead, and a review of the Biomass CCI reports - Product Validation Plan and Uncertainty Budget, was submitted as part of other CMUG work.

Publications

None so far, but a paper on the evaluation of modelled seasonality in vegetation is planned.

Interactions with the ECVs used in this experiment

In the first 12 months of this phase of CMUG work there have been interactions with the LST, AGB, SM and LC CCI ECV projects at the quarterly CSWG meetings and the Integration meetings. Contact outside that has been with LST who have already produced a beta dataset, and AGB (by email) to discuss data specifications and access, and the wider question of coordinated work on using the AGB data in a land surface climate model. Interactions with SM and LC have been to learn about the continuation datasets they will be producing in CCI+. Interactions with the LS3MIP, C4MIP, LUMIP and Decadal Climate Prediction projects are planned for 2020.

Consistency between data products

This section will provide a record of any inconsistencies found between ECV products, and will be completed in the next version of this report.

Recommendations to the CCI ECV teams

To be completed in next version of this report.



4.11 Assess the land-surface interaction related biases in AMIP simulations with CCI and other products

Lead partner: IPSL

Author: Frederique Cheruy

Aim

The aim of this research is to identify biases in the surface state and surface fluxes in AMIP simulations and understanding the origin of these biases in present day simulations (temperature, albedo, fluxes). It will address the following scientific question: What is the potential for exploring multiple satellite derived products to try to relate existing and identified biases (surface state and surface fluxes) to missing or incorrectly represented processes, thus offering solutions for model improvement by revisiting the process representation?

Summary of Work and Results

The soil-moisture atmosphere couplings have been assessed for the IPSL-CM in AMIP configuration. An evaluation of the snow cover has been done with alternative products since the snow product was not yet available. The new versions of atmospheric and soil physics of the IPSL model implemented for CMIP6 leads to an image of the interactions between soil moisture and atmosphere that is more consistent with observations. This is particularly true in “hot-spot” regions of strong land-atmosphere coupling and for the driest soils where evaporation and precipitation distributions are closer to those of the observations for the driest soil moisture quartile. Spurious multi-modality in the regional distribution of the superficial soil moisture has been documented over some regions, and is probably related to contrasted field capacities and wilting points as a function of soil texture in our land surface model. This multi-modality is not present in the CCI product, which needs to be investigated by comparing SSM spatio-temporal variability in the three ESA CCI SM products: active (in % saturation), passive (in m³/m³) and combined (which imposes the dynamic range of the GLDAS-Noah SSM product, making this product unfit for bias and RMSD analyses, *cf.* Dorigo et al, 2017). The effect of input soil texture on the distributions of SSM in the ISPL model can also be explored owing to a set of idealized simulations with uniform soil texture over land, recently performed for the Soil Parameter MIP international project (Tafasca et al., 2020).

Publications

None so far, but a paper on the results is planned if they are of sufficient interest.



Interactions with the ECVs used in this experiment

In the first 12 months of this phase of CMUG work there have been interactions with the LST and Snow CCI ECV projects at the quarterly CSWG meetings and the Integration meetings. Contact outside that has been with LST who have already produced a beta dataset. Interactions with the LS3MIP, SPMIP, AMIP, HighResMIP and SnowMIP projects are planned for 2020.

Consistency between data products

This section will provide a record of any inconsistencies found between ECV products, and will be completed in the next version of this report.

Recommendations to the CCI ECV teams

To be completed in next version of this report.



5. References

Boer J., *et al.*, 2016: The Decadal Climate Prediction Project (DCPP) contribution to CMIP6, *Geosci. Model Dev.*, 9, 3751–377

Dorigo, W., Wolfgang Wagner, Clement Albergel, Franziska Albrecht, Gianpaolo Balsamo, Luca Brocca, Daniel Chung, Martin Ertl, Matthias Forkel, Alexander Gruber, Eva Haas, Paul D. Hamer, Martin Hirschi, Jaakko Ikonen, Richard de Jeu, Richard Kidd, William Lahoz, Yi Y. Liu, Diego Miralles, Thomas Mistelbauer, Nadine Nicolai-Shaw, Robert Parinussa, Chiara Pratola, Christoph Reimer, Robin van der Schalie, Sonia I. Seneviratne, Tuomo Smolander, Pascal Lecomte (2017). ESA CCI Soil Moisture for improved Earth system understanding: State-of-the art and future directions, *Remote Sensing of Environment*, Volume 203, Pages 185-215, <https://doi.org/10.1016/j.rse.2017.07.001>.

Meier, W., F. Fetterer, M. Savoie, S. Mallory, R. Duerr, and J. Stroeve, 2013: NOAA/NSIDC Climate Data Record of Passive Microwave Sea Ice Concentration, version 2. National Snow and Ice Data Center, Boulder, CO, accessed 9 December 2015, <https://doi.org/10.7265/N55M63M1>.

Olonscheck, D. & Notz, D. (2017), Consistently Estimating Internal Climate Variability from Climate Model Simulations. *Journal of Climate* 30, 9555–9573, doi:10.1175/JCLI-D-16-0428.1.

Tafasca, S., Ducharne, A., and Valentin, C. (2020). Weak sensitivity of the terrestrial water budget to global soil texture maps in the ORCHIDEE land surface model, *Hydrol. Earth Syst. Sci. Discuss.*, DOI: 10.5194/hess-24-3753-2020

Trenberth, K. E. & Shea, D. J. (2006) Atlantic hurricanes and natural variability in 2005. *Geophysical Research Letters* 33, L12704, doi:10.1029/2006GL026894

Wilks, D. (2019). *Statistical Methods in the Atmospheric Sciences*, 4th Edition. Elsevier, pp 840. ISBN: 9780128158234